JACS
JOURNAL OF THE AMERICAN CHEMICAL SOCIETY
Article
pubs.acs.org/JACS

Noncentrosymmetric Inorganic Open-Framework Chalcohalides with Strong Middle IR SHG and Red Emission: $Ba_3AGa_5Se_{10}Cl_2$ (A = Cs, Rb, K)

Peng Yu,[†,‡] Liu-Jiang Zhou,[†,‡] and Ling Chen*[,†]

[†]Key Laboratory of Optoelectronic Materials Chemistry and Physics, Fujian Institute of Research on the Structure of Matter, Chinese Academy of Sciences, Fuzhou, Fujian 350002, People's Republic of China

[‡]Graduate University, Chinese Academy of Sciences, Beijing 100039, People's Republic of China

Supporting Information

ABSTRACT: Novel SHG effective inorganic open-framework chalcohalides, $Ba_3AGa_5Se_{10}Cl_2$ (A = Cs, Rb and K), have been synthesized by high temperature solid state reactions. These compounds crystallize in the tetragonal space group $I\bar{4}$ (No.82) with $a = b = 8.7348(6) - 8.6341(7)$ Å, $c = 15.697(3) - 15.644(2)$ Å, $V = 1197.6(3) - 1166.2(2)$ Å^3 on going from Cs to K. The polar framework of $^3_\infty[Ga_5Se_{10}]^{5-}$ is constructed by nonpolar $GaSe_4^{5-}$ tetrahedron (T1) and polar supertetrahedral cluster $Ga_4Se_{10}^{8-}$ (T2) in a zinc-blende topological structure with Ba/A cations and Cl anions residing in the tunnels. Remarkably, $Ba_3CsGa_5Se_{10}Cl_2$ exhibits the strongest intensity at 2.05 μm (about 100 times that of the benchmark $AgGaS_2$ in the particle size of 30−46 μm) among chalcogenides, halides, and chalcohalides. Furthermore, these compounds are also the first open-framework compounds with red photoluminescent emissions. The Vienna ab initio theoretical studies analyze electronic structures and linear and nonlinear optical properties.

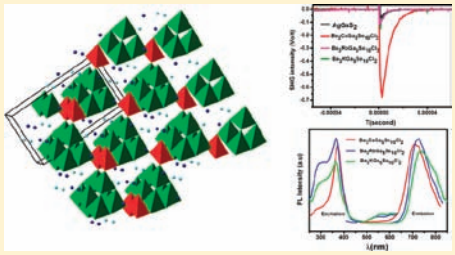

INTRODUCTION

Mid- and far-IR (>2 μm, MFIR) nonlinear optical (NLO) materials as coherent and tunable sources have become increasingly important and have become urgently needed in the last several decades for scientific and technological applications, especially in the fields of photochemistry, explosives detection, spectroscopy, and frequency metrology, photomedicine, industrial process control, and information technology.[1−3] Unfortunately, the well-known UV and visible-region NLO materials, such as borate,[4−9] phosphate,[10,11] and metal oxide,[12,13] are restricted in the MFIR regions because their metal−oxygen bond absorption bands and the overtones lower the efficiencies and optical transparencies.[14−16] The commercial MFIR NLO materials are $AgGaS_2$,[17,18] $AgGaSe_2$,[19−21] and $ZnGeP_2$,[22] but each of them suffers some drawbacks, such as, low laser damage threshold or two-photon absorption. Therefore, the discovery of effective MFIR NLO materials is of great interest, which has led to the discovery of many new compounds with large NLO coefficients and wide transparencies in MFIR regions, such as $LiGaS_2$,[23−25] $BaGa_4S_7$,[26] $BaGa_4Se_7$,[27] $Li_2Ga_2GeS_6$,[28] $A_2Hg_3M_2S_8$ (A = K, Rb; M = Ge, Sn),[29] $A_2P_2Se_6$ (A = K, Rb),[30] $A_3Ta_2AsS_{11}$ (A = K, Rb),[31,32] $HgGa_2S_4$,[33] $CsGeCl_3$,[34] $CsCdBr_3$,[35] $Cs_2Hg_3I_8$,[36] $(Hg_6P_3)(In_2Cl_9)$, $(Hg_8As_4)(Bi_3Cl_{13})$,[37] NaI_3O_8,[38] and $Mg(IO_3)_2$.[39] In comparison, NLO active chalcohalides are extremely rare—only three compounds $LaCa_2GeS_4Cl_3$,[40] $(Sb_7S_8Br_2)(AlCl_4)_3$,[41] and $(K_3I)[SmB_{12}(GaS_4)_3]$,[42] are known—and unfortunately show inadequate optical transparencies and relatively low SHG efficiencies.

The primary requirement for the NLO materials is a noncentrosymmetric (NCS) crystal structure and the common strategy of design NCS structure is to organize the asymmetric building units, including d^0 transition metal-centered polyhedron (e.g., Ti^{4+}, Nb^{5+}, W^{6+}, Ta^{5+}, etc.),[10−13,31,32] stereoactive lone-pair cation (e.g., Se^{4+}, Sb^{3+}, Te^{4+}, As^{3+}, I^{5+}, etc.),[12,13,31,32,43−45] or NCS π-orbital system (e.g., BO_3^{3-} and $B_3O_6^{3-}$).[4,5,46] Transition metals, such as Nb^{5+}, Ta^{5+}, or Zr^{6+}, integrate with lone-pair units (e.g., PS_3^{3-}, PSe_3^{3-}, AsS_3^{3-}, or $AsSe_3^{3-}$) to yield compounds with strong SHG response, for instance $AZrPQ_6$ (A = K, Rb, Cs; Q = S, Se) and $A_3M_2AsQ_{11}$ (A = K, Rb, Cs; M = Nb, Ta; Q = S, Se).[31,32,47] On the one hand, we notice that the tetrahedral anion GaQ_4^{5-} is the structure building unit as well as the property (polarity) unit of many excellent IR NLO compounds, such as benchmark $AgGaS_2$,[17,18] $AgGaSe_2$,[19−21] $LiGaS_2$,[23−25] $BaGa_4S_7$,[26] $BaGa_4Se_7$,[27] $Li_2Ga_2GeS_6$,[28] and Ln_4GaSbS_9.[44] On the other hand, we previously found the significant contribution of I^- anion to the overall SHG in an excellent NLO material $Pb_2B_5O_9I$.[48] Therefore, we consider to combine halogen and GaQ_4 anions in a single compound may be a new route to discover excellent NLO compound. Here, we introduce Cl^- into Ga/Se system and discover three novel NLO active polar open framework chalcohalides $Ba_3AGa_5Se_{10}Cl_2$ (A = Cs, Rb and K). These are the first open framework chalcohalides showing strong powder SHG response at 2.05 μm with intensities about 100, 20, and

Received: October 16, 2011
Published: January 11, 2012

   dx.doi.org/10.1021/ja209711x | J. Am. Chem.Soc. 2012, 134, 2227−2235

10 times that of commercial $AgGaS_2$ in the particle size of 30−46 μm and large transparency regions (0.89−25 μm). Remarkably, $Ba_3CsGa_5Se_{10}Cl_2$ shows the strongest SHG intensity among chalcogenides, halides, and chalcohalides to date. Compared with quite a number of organic−inorganic supertetrahedral open framework materials with photoluminescence,[49−54] such interesting compounds emit red light, which extends the emission range of the open framework photoluminescence. The theoretical studies reveal the roles of the GaS_4 building unit and the Cl^- anion, as expected.

EXPERIMENTAL SECTION

Synthesis. All of the manipulations were performed in an Ar-filled glovebox with controlled oxygen and moisture levels below 0.1 ppm. Ba (99%, Alfa Aesar) was first brushed to remove the oxidized layer before using. Ga, Nb, Se, $BaCl_2$ (higher than 99.9%) purchased from Alfa Aesar China (Tianjin) Co., Ltd. and KCl, RbCl, CsCl (99.5%) purchased from XinJiang Research Institute. The reaction was carried out in a graphite crucible sealed in an evacuated fused-silica tube, and heated in a tube furnace with controlled temperature. The orange-yellow crystals of $Ba_3CsGa_5Se_{10}Cl_2$ were originally obtained from the reaction of Ba:Ga:Nb:Se = 3:1:3:13 with a total weight of about 300 mg plus extra 200 mg of CsCl as a flux. The reactants were heated to 1000 °C in 60 h and dwelled for 100 h, cooled to 450 at 5 °C/h before switching off the furnace. The subsequent single crystal analyses revealed that Nb did not react, CsCl served as a reactant and $Ba_3CsGa_5Se_{10}Cl_2$ instead of the hypothetic "$Ba_3GaNb_3Se_{13}$" was produced. Then, the optimal synthetic conditions of $Ba_3AGa_5Se_{10}Cl_2$ (A = Cs, Rb and K) were established. Pure phases were produced via a stoichiometry mixture of Ba/Ga/Se/ACl/$BaCl_2$ = 5:10:20:2:1 that were heated to 850 °C in 50 h, and kept for 100 h and then slowly cooled at 5 °C/h to 450 °C before turning off the furnace. (Figure S1 of the Supporting Information, SI) Note that ACl and $BaCl_2$ salts served as reactants instead of mere fluxes in these reactions. These orange-yellow compounds are stable in air at room temperature for several months.

Single Crystal Structure Determinations. Single crystal X-ray diffraction data were collected with the aid of a Mercury CCD automatic diffractometer equipped with a graphite-monochromated MoKα radiation (λ = 0.71073 Å) at room temperature. The data were corrected for Lorentz factors, polarization, air absorption, and absorption due to variations in the path length through the detector faceplate. The SADABS program performed absorption correction based on a multiscan technique.[55] The nocentrosymmetric space group $I\bar{4}$ (No. 83) was determined according to systematic absences, E-value statistics ($|E^2 - 1|$ values are 0.737, 0.729, and 0.744 for Cs-, Rb- and K-compounds, respectively, which are close to the theoretical 0.736 for a noncentrosymmetric structure) and subsequently successful refinements of the crystal structure. All structures were solved by the direct methods and refined by full-matrix least-squares fitting on F^2 by SHELX-97.[56] For example, the first run of a routine refinement of the initial structure generated an "un-balanced" formula of "$Ba_4Ga_5Se_{10}Cl_2$" with $R1$ = 3.57%, $R2$ = 9.84%. The subsequent EDS data suggested the existence of K. Thus, potassium was assigned to coshare the 8g site with fixed occupancies of 0.25 K and 0.75 Ba, which yielded a neutral formula of "$Ba_3KGa_5Se_{10}Cl_2$" $\equiv (Ba^{2+})_3(K^+)(Ga^{3+})_5(Se^{2-})_{10}(Cl^-)_2$, and $R1$ and $R2$ converged to better values of 0.0220 and 0.0448. In comparison, the free occupancy refinement on 8g site generated similar occupancies, K: 0.231(2), Ba: 0.769(2) and comparable R values (0.0215, 0.0440). Similar situations were found in Rb-compound, in which the corresponding FREE refined occupancies were Rb 0.279(3) and Ba 0.721(3), with R values of 0.0145, 0.0398 vs constraint refinement: 0.0147, 0.0399. In case of Cs-compound, since the similar atomic weight of Ba and Cs, it was not surprise that the free refined occupancies of Ba and Cs were half and half, 0.501(4) and 0.499(4). (SI Table S3) Because no metal−metal, Se−Se or Cl−Cl bond was involved, and the existence of alkali metal was confirmed by the EDS results, (SI Figure S2) the neutral formula "$Ba_3KGa_5Se_{10}Cl_2$" was considered to be rational. The crystallographic details are listed in Tables 1, 2, SI S1, and the atomic positions and thermal parameters are given in Tables 3, SI S2.

Table 1. Crystal Data and Structure Refinements for $Ba_3AGa_5Se_{10}Cl_2$ (A = Cs, Rb, and K)[a]

formula	$Ba_3CsGa_5Se_{10}Cl_2$	$Ba_3RbGa_5Se_{10}Cl_2$	$Ba_3KGa_5Se_{10}Cl_2$
fw	1754.02	1706.56	1660.19
crystal system	tetragonal	tetragonal	tetragonal
crystal color	orange yellow	orange yellow	orange yellow
space group	$I\bar{4}$ (NO. 82)	$I\bar{4}$ (NO. 82)	$I\bar{4}$ (NO. 82)
$a = b$ (Å)	8.7348(6)	8.6629(4)	8.6341(7)
c (Å)	15.697(3)	15.6379(13)	15.644(2)
V (Å^3)	1197.6(3)	1173.56(12)	1166.2(2)
Z	2	2	2
D_c (g·cm^{-3})	4.864	4.830	4.726
μ (mm^{-1})	35.087	25.998	26.660
GOOF on F^2	1.021	0.939	0.936
Flack parameter	0.000(16)	0.00(2)	0.052(19)
R_1, wR_2 ($I > 2\sigma(I)$)[a]	0.0192, 0.0342	0.0170, 0.0318	0.0247, 0.0442
R_1, wR_2 (all data)	0.0203, 0.0346	0.0181, 0.0320	0.0275, 0.0448
largest diff peak/hole, e Å^{-3}	0.516/−0.573	0.405/−0.474	0.671/−0.579

[a] $R1 = \sum||F_o| - |F_c||/\sum|F_o|$ for $F_o^2 > 2\sigma(F_o^2)$; $wR2 = \sum[w(F_o^2 - F_c^2)]/\sum[w(F_o^2)^2]^{1/2}$, where $w = 1/[\sigma^2F_o^2 + (AP)^2 + BP]$, and $P = (F_o^2 + 2F_c^2)/3$.

Table 2. Selected Bond Lengths (Å) of $Ba_3CsGa_5Se_{10}Cl_2$

$Ba_3CsGa_5Se_{10}Cl_2$			
Ba/Cs−Cl2	3.1131(4)	Ba/Cs−Se3	3.7478 (9)
Ba/Cs−Cl1	3.1969(5)	Ba/Cs−Se3	4.01
Ba/Cs−Se1	3.4914 (6)	Ga2−Se1 × 4	2.4111 (5)
Ba/Cs−Se1	3.6745 (8)	Ga1−Se1	2.3928(7)
Ba/Cs−Se1	3.87	Ga1−Se2	2.4039(7)
Ba/Cs−Se2	3.3894(7)	Ga1−Se2	2.4083(7)
Ba/Cs−Se2	3.6780(7)	Ga1−Se3	2.3858(8)
Ba/Cs−Se2	3.7518 (7)		

Powder X-ray Diffraction. The powder XRD patterns were collected at room temperature on a Rigaku DMAX 2500 diffractometer, using monochromatized Cu Kα radiation. Data were collected in the range 2θ = 10−85° with scan steps of 0.05°. The measured X-ray powder diffraction patterns of the samples are in good agreement with the simulated ones calculated from the single crystal data shown in SI Figure S1.

Elemental Analysis. Semiquantitative microprobe analyses on the compounds were performed with the aid of a field emission scanning electron microscope (FESEM. JSM6700F) equipped with an energy dispersive X-ray spectroscope (EDX, Oxford INCA). The energy dispersive spectra (EDS) taken on visibly clean surfaces of the sample proved the presence of Ba, Cs/Rb/K, Ga, Se, and Cl. ($Ba_{2.8}Cs_{0.8(1)}Ga_{4.8(8)}Se_{11.2(2)}Cl_{2.2(2)}$, $Ba_{2.8}Rb_{0.9(2)}Ga_{4.5(9)}Se_{11.8(13)}Cl_{2.3(4)}$, and $Ba_{2.8}K_{0.8(1)}$ $Ga_{4.8(6)}Se_{11.7(2)}Cl_{2.3(5)}$) (SI Figure S2)

UV−vis-NIR Diffuse Reflectance Spectra and Infrared Spectra. The UV−vis-NIR diffuse reflectance spectra were measured on a Perkin−Elmer Lambda 900 UV−vis-NIR spectrometer equipped with an integrating sphere over a 190−2500 nm wavelength range at room temperature and a $BaSO_4$ plate as a reference, on which the finely ground samples were coated. The absorption spectrum was calculated from the reflection spectrum via the Kubelka−Munk function: $\alpha/S = (1 - R)^2/2R$, in which α was the absorption coefficient, S was the scattering coefficient, and R was the reflectance.[57] The IR spectra were measured by using a Nicolet Magana 750 FT−IR spectrophotometer in the range of 2.5−25 μm and samples were

dx.doi.org/10.1021/ja209711x | J. Am. Chem.Soc. 2012, 134, 2227−2235

Table 3. Atomic Coordinates and Equivalent Isotropic Displacement Parameters of $Ba_3CsGa_5Se_{10}Cl_2$

atom	oxidation	Wyckoff	occ	x	y	z	U (eq)
Ba	+2	8g	0.75	0.1303(1)	0.2614(1)	0.3864(1)	0.028(1)
Cs	+1	8g	0.25	0.1303(1)	0.2614(1)	0.3864(1)	0.028(1)
Ga1	+3	8g	1	0.3084(1)	0.0995(1)	0.1655(1)	0.014(1)
Ga2	+3	2a	1	0	0	0	0.014(1)
Se1	−2	8g	1	0.1206(1)	0.2093(1)	0.0743(1)	0.017(1)
Se2	−2	8g	1	0.4127(1)	0.3112(1)	0.2409(1)	0.020(1)
Se3	−2	4f	1	0	0.5	0.5710(1)	0.029(1)
Cl1	−1	2c	1	0	0.5	0.2500(1)	0.039(1)
Cl2	−1	2b	1	0	0	0.5	0.047(1)

[a] U_{eq} is defined as one-third of the trace of the orthogonalized U_{ij} tensor

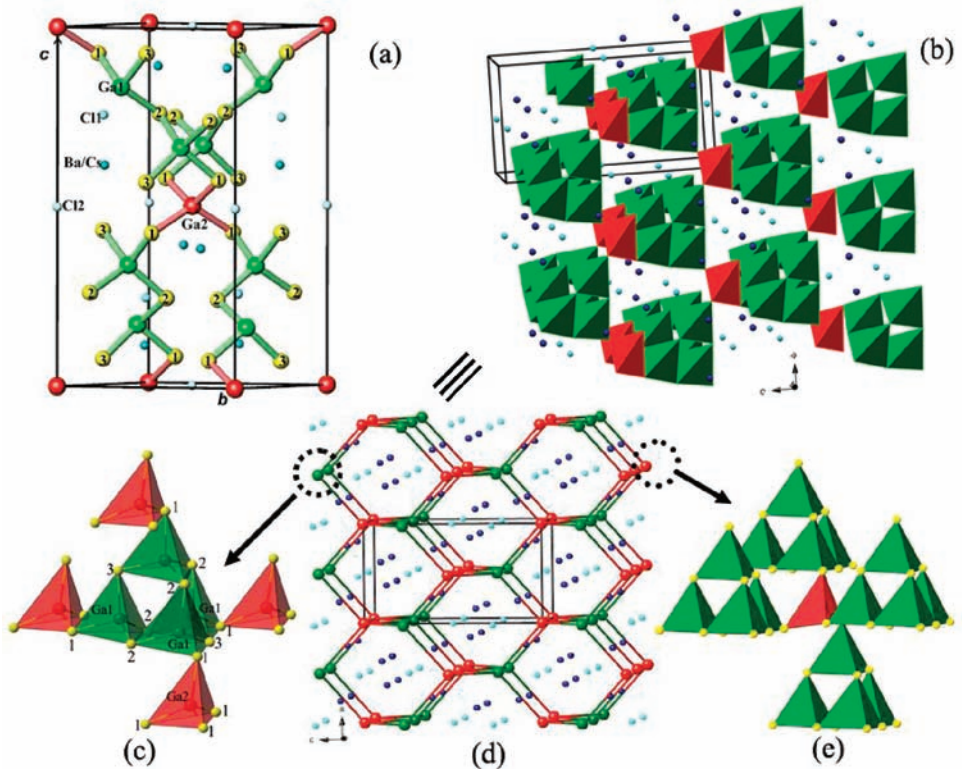

Figure 1. (a) Unit cell of $Ba_3CsGa_5Se_{10}Cl_2$ with atom marked. (b) Structure viewed approximately down the *b* axis with unit cell marked to emphasize the T1−T2 hybrid covalent framework. (c) Four T1 tetrahedra are linked together by a T2 cluster. (d) Topological representation viewed down approximately the *b* axis with unit cell outlined. (e) Four T2 clusters are linked together by a T1 cluster. Light blue: Cl anion, dark blue: Cs/Ba cation. Red: T1 tetrahedron $Ga2Se_4^{5-}$ and Ga2, green: T2 supertetrahedral cluster $Ga1_4Se_{10}^{8-}$ and Ga1.

ground and pressed with KBr into transparent pellets, which suggest that no obvious FT-IR absorption peak of the compounds appear in the range of 2.5−25 μm.

Second Harmonic Generation (SHG) Measurements. The SHG response was measured on powdered samples by using the Kurtz and Perry method with 2.05 μm Q-switch laser.[58] All of the samples were ground and sieved into a series of distinct particle size ranges of 30−46, 46−74, 74−106, 106−150, and 150−210 μm, respectively, which were pressed into a disk with diameter of 8 mm that was put between glass microscope slides and secured with tape in a 1-mm thick aluminum holder, and powdered $AgGaS_2$ sample used as the reference was sieved into the same size range.

Photoluminescence Measurement. Detailed photoluminescence spectra were recorded by a FLS920 spectrofluorometer with the range of 190−1700 nm on the powdered samples at room temperature.

Electronic Structure Calculations. The calculation models were built in *P*1 symmetry to avoid the fractional occupancies of Ba and A atom at 8*g* site. The geometrical optimizations based on density functional theory (DFT) were carried out utilizing the Vienna ab initio simulation package (VASP)[59−61] and the projected augmented wave (PAW) method, in which the Perdew-Burke-Ernzerhof (PBE)[62] type exchange-correlation was adopted. An energy cutoff of 364 eV and a 3 × 3 × 3 *k*-point grid were employed in the geometrical optimizations, by which the optimized lattice parameters of the compounds were a = 8.9750 Å, b = 8.8291 Å, and c = 15.8864 Å for Cs-compound, a = 8.8914 Å, b = 8.8004 Å, and c = 15.8421 Å for Rb-compound, and a = 8.7703 Å, b = 8.8450 Å, and c = 15.8168 Å for K-compound, which agreed well with the experimental values (Table 1).

The electronic band structures were also calculated by VASP, the generalized gradient approximation (GGA)[63] was chosen as the exchange-correlation functional and a plane wave basis with the projector-augmented wave (PAW) potentials was used. The plane-wave cutoff energy of 280 eV and the threshold of 10^{-5} eV were set for the self-consistent-field convergence of the total electronic energy. The interactions between the ionic cores and the electrons were described by the norm-conserving pseudopotential.[64] Ba $5s^25p^66s^2$, Cs $5s^25p^66s^1$, Rb $4s^24p^65s^1$, K $3s^23p^64s^1$, Ga $4s^24p^1$, Se $4s^24p^4$, and Cl $3s^23p^5$ were

dx.doi.org/10.1021/ja209711x | J. Am. Chem.Soc. 2012, 134, 2227−2235

treated as valence electrons. And the numerical integration of the Brillouin zone was performed utilizing a 7 × 7 × 7 *k*-point Grid sampling for the three compounds. The Fermi level (E_f = 0 eV) was selected as the reference.

Optical Properties Calculations. More than 250 empty bands were used in optical property calculations and scissors operators of −0.14, −0.16, and −0.19 were applied for Cs-, Rb-, and K-compounds, respectively. The 7 × 7 × 7 *k*-point grids were applied. Complex dielectric function $\varepsilon(\omega) = \varepsilon_1(\omega) + i\varepsilon_2(\omega)$ were calculated, of which the imaginary part $\varepsilon_2(\omega)$generated other optical constants via the Kramers−Kroning transform.[65,66] The static and dynamic second-order nonlinear susceptibilities $\chi^{abc}(-2\omega,\omega,\omega)$ were calculated based on the so-called length-gauge formalism by Aversa and Sipe.[67,68] More details are listed in the SI.

RESULTS AND DISCUSSION

Crystal Structure. As the first inorganic open-framework compounds, $Ba_3AGa_5Se_{10}Cl_2$ (A = Cs, Rb and K) represent a new type of nocentrosymmetric structure that is constructed by supertetrahedral clusters in the tetragonal space group $I\bar{4}$ with $a = b$ = 8.7348(6) − 8.6341(7) Å, c = 15.697(3) − 15.644(2) Å on going from Cs to K. As shown in Figure1a,b, the three-dimensional anionic covalent framework of $^3_\infty[Ga_5Se_{10}]^{5-}$ is interpenetrated by Ba^{2+}/Cs^+ cations and Cl^- anions. Such an anionic framework crystallizes in a zinc-blende topological structure in which all the Zn and S sites are alternately substituted by supertetrahedral $Ga_4Se_{10}^{8-}$ cluster (T2) and tetrahedron $GaSe_4^{5-}$ (T1). (Figure 1e) Four aligned Ga1Se_4 tetrahedra constitute a T2 supertetrahedral cluster via corner sharing (Se2, Se3) that is further linked with T1 tetrahedron Ga2Se_4^{5-} by common Se1 corner. (Figure1a,c,d) The slightly distorted Ga2Se_4 tetrahedron (T1) has mirror symmetry with Ga2−Se1 bond of 2.4111(5) Å and Se−Ga2−Se angles ranging from 103.5 to 122.1°. In comparison, the distortion of Ga1Se_4 tetrahedron of T2 is distinct with Ga1−Se bond lengths ranging from 2.3858(8) to 2.4083(7) Å and Se−Ga2−Se angles varying from 103.2 to 112.5°. These data are in agreement with those in related gallium selenides, such as Ga_2Se_3 (2.38−2.39 Å, 100.1−113.8°);[69] $AgGaSe_2$ (2.443(1) Å, 108.2−111.9°);[19−21] $BaGa_4Se_7$ (2.361(2)−2.488(2) Å, 98.8−126.2°);[27] $LiGaSe_2$ (2.38−2.40 Å, 106.7−109.6°).[70] The T1 cluster is nonpolar because of its mirror symmetry, however, the T2 supertetrahedral cluster is polar, because its constituent Ga1Se_4 tetrahedron as well as the whole T2 cluster itself only show C_1 symmetry. Thus, the overall polarity of the compound that leads to the strong SHG response as discussed below, comes merely from the polar T2 supertetrahedral building units. In spite of crystallizing with the inorganic counter cations, the title compounds show similar supertetrahedron connection mode as the known organic−inorganic hybrid open-frameworks, such as, the T5-T3 connection in $(In_{34}S_{54})(In_{10}S_{18})(C_{11}H_{24}N_2)_6$,[71] and T1-T2 connection in $(Me_4N)_2M[Sn_4Se_{10}]$ (M = Mn^{2+}, Fe^{2+}, Co^{2+}, Zn^{2+}).[72]

The single crystal data refinement and EDS results reveal a disorder of Ba and alkali metal (A = Cs, Rb or K) atoms on 8*g* site driven by the charge neutrality requirement as discussed above, similar Ba/A atom disorder was reported in (Ba, K)VSe_3.[73] As shown in SI Figure S3, Tables 2 and SI S1, the bonding distances of Ba/A−Cl are 3.0831(6) and 3.1969(5) Å, and Ba/A−Se ranges from 3.3428(9) Å to 3.87 Å, which are comparable with the Ba−Se bond lengths in $BaGa_4Se_7$ (3.429(2) Å),[27] and $BaLaSb_2Se_6$ (3.2751(8)−3.8079(8) Å).[74]

UV−vis-NIR and Infrared Diffuse Reflectance Spectra. The IR spectra and diffuse-reflectance UV/vis/near-IR spectra indicated broad transparent regions of 0.89−25 μm (Figure 2), 0.65−25 μm (SI Figure S4a), and 0.86−25 μm (SI Figure S4b)

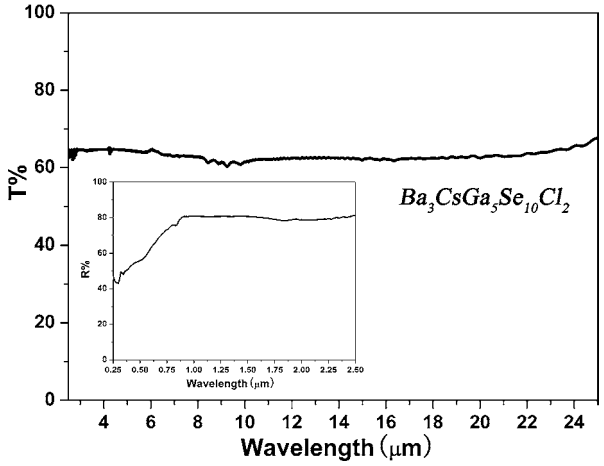

Figure 2. Reflection (inset panel) and FT-IR spectra of $Ba_3CsGa_5Se_{10}Cl_2$.

for Cs, Rb, and K-compounds, respectively. These are comparable with those of powdered $AgGaS_2$ (0.15−23 μm) (SI Figure S4c), powdered $BaGa_4Se_7$ (up to 18 μm),[27] powdered Sm_4GaSbS_9 (1.75−25 μm),[44] and single crystal $LiGaSe_2$ (0.37−13.2 μm).[70] Therefore, the title compounds exhibit considerable broad transparent range in the MFIR region that run across the important band ranges of atmospheric transparent windows (3−5 and 8−14 μm) and may be possible candidates for MFIR NLO materials because transparency in MFIR region is an additional criterion for applications.

In agreement with their orange-yellow colors, the optical band gaps for Cs, Rb and K-compounds are approximately 2.08 (Figure 3), 2.05 (SI Figure S5a), and 2.04 eV (SI Figure S5b).

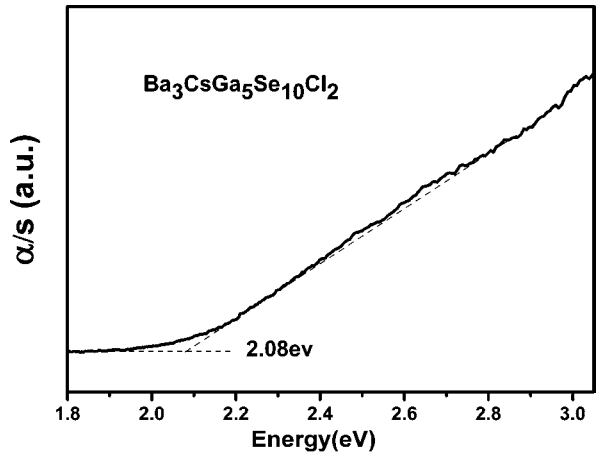

Figure 3. UV−vis diffuse reflectance of $Ba_3CsGa_5Se_{10}Cl_2$.

These data are smaller than those of $AgGaS_2$ (2.62 eV),[75] $BaGa_4S_7$ (3.54 eV),[26] β-$LaGaS_3$ (2.5 eV),[76] $LiGaS_2$ (3.87 eV),[70] $LiGaSe_2$ (3.34 eV),[70] Sm_4GaSbS_9 (2.23 eV),[44] $BaGa_4Se_7$ (2.64 eV),[27] and $(K_3I)[SmB_{12}(GaS_4)_3]$ (2.35),[42] but wider than those of $AgGaSe_2$ (1.8 eV)[75] and $ZnGeP_2$ (1.75 eV),[22] which indicates that the laser-induced damage threshold of the title compounds may be relatively higher than those of $AgGaSe_2$[75]

dx.doi.org/10.1021/ja209711x | J. Am. Chem.Soc. 2012, 134, 2227−2235

and $ZnGeP_2$[22] because the band gap has great effect on the laser-induced damage threshold and generally bigger band gap leads to the higher laser-induced damage threshold. Thus, $Ba_3AGa_5Se_{10}Cl_2$ (A = Cs, Rb and K) compounds may represent a new family of MFIR NLO materials.

NLO Properties. The SHG properties of powdered $Ba_3AGa_5Se_{10}Cl_2$ (A = Cs, Rb, and K) have been measured using the Kurtz and Perry method with 2.05 μm Q-switch laser and $AgGaS_2$ as a reference. The plots of the SHG signals as a function of particle size measured on ground crystals suggest type-I nonphase-matchable behaviors at 2.05 μm. (Figure 4)

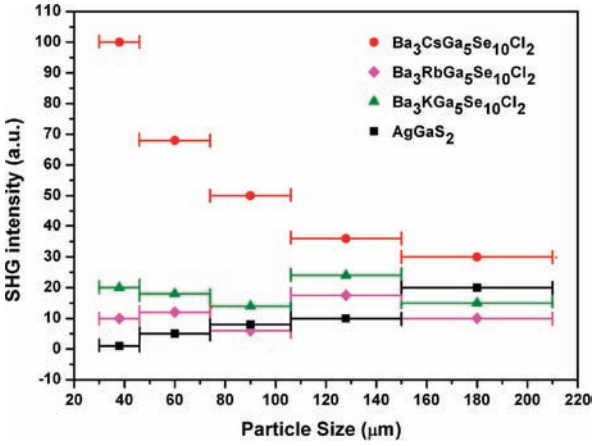

Figure 4. Phase-matching curves, i.e., particle size vs SHG intensity, for $Ba_3AGa_5Se_{10}Cl_2$ (A = Cs, Rb, and K).

The related compound $[Sb_7S_8Br_2](AlCl_4)_3$ also shows type-I nonphase-matchability.[41,77−79] The SHG intensities for $Ba_3CsGa_5Se_{10}Cl_2$, $Ba_3RbGa_5Se_{10}Cl_2$, and $Ba_3KGa_5Se_{10}Cl_2$ are about 100, 20, and 10 times that of $AgGaS_2$ in the particle size of 30−46 μm (Figure 4). Remarkably, $Ba_3CsGa_5Se_{10}Cl_2$ shows the highest intensity among chalcogenides, halides and chalcohalides at 2.05 μm. In comparison, some selected examples are listed as follows: $[Sb_7S_8Br_2](AlCl_4)_3$ (1/3 × KDP, in the particle size of 45.5 ± 7.5 μm, at λ = 700 nm),[41] $(Hg_8As_4)(Bi_3Cl_{13})$ (1.2 × $AgGaS_2$ at λ = 2.05 μm),[37] $BaGa_4S_7$ (0.96 × $AgGaS_2$ at λ = 2.05 μm).[25] Generally, the phase matchability is closely related to and varies with the wavelength, for example, $AgGaSe_2$ is phase matchable only in the range 3800−12 400 nm.[80] Hence, the title compounds may be phase matchable in a different wavelength range. Besides, the measurements also indicate that the alkali metal has a significant influence on the SHG intensity. (Figure 4)

Photoluminescence Properties. The excitation and emission spectra are shown in Figure 5. With excitation wavelengths of λ_{ex} = 373, 367, and 364 nm, broad emission peaks with maxima are found at λ_{em} = 711, 726, and 731 nm, respectively.

Strong photoluminescence is commonly found in open-framework compounds, such as 360−420 nm emissions in phosphates,[49] 400−440 nm emissions in germinates,[49] 440−500 nm emissions in gallium sulfides,[50] and 520−570 nm in indium sulfides.[51,52] It is the first time that the 711−731 nm luminescent output is observed in the open-framework structure, which extends the emission region in the open-framework photoluminescence. Compared to the reported organic−inorganic hybrid open-frameworks, the inorganic title compounds are superior at least in thermal stability. According

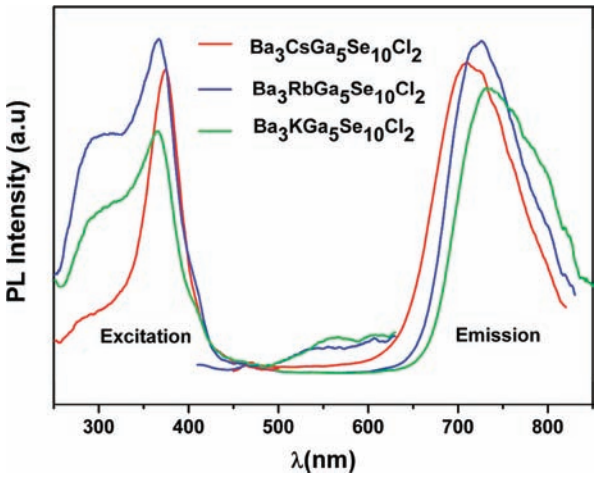

Figure 5. Photoluminescence spectra of $Ba_3AGa_5Se_{10}Cl_2$ (A = Cs, Rb and K).

to Feng, the luminescent mechanism for the open-framework materials was not unambiguously known at this stage and the reason why such materials without metal activators still can emit luminescence due to the highly negatively charged inorganic framework and the presence of protonated guest amine molecules.[49] The title compounds exclude the influence of the organic guest molecule influence. However, the photoluminescent phenomena of the non−lanthanide oxides and chalcogenides without metal activators are often closely related to the delocalization of electrons in various defect levels or energy states lying within the band gap of the materials, such as, $CdGa_2Se_4$ exhibit strong photoluminescent emission due to the presence of the point defects originating from cadmium vacancies, selenium vacancies, cadmium interstitials, and selenium interstitials.[81] Therefore, it is possible that the excited electrons of the title compounds originate from the existence of various kinds of lattice defects for instance the point defects and color centers, which is in agreement with the poor luminescence efficiency. (The overall quantum yields are $\Phi_{overall}$ = 1.13, 0.74, and 0.87%, for Cs, Rb and K-compounds, respectively.)

Electronic Structure Calculations. The band structures are presented in SI Figure S6, and the lowest conduction band (LCB) energy and the highest valence band (HVB) energy of the first Brillouin zone are listed in SI Table S4. Compounds $Ba_3CsGa_5Se_{10}Cl_2$ and $Ba_3RbGa_5Se_{10}Cl_2$ have indirect band gaps of 2.22 and 2.21 eV, whereas $Ba_3KGa_5Se_{10}Cl_2$ has a direct band gap of 2.23 eV. These values are larger than the experimental observations (2.08, 2.05, and 2.04 eV) owning to the inaccurately describing of the eigenvalues of the electronic states in GGA. Subsequently, scissor values of −0.14, −0.16, and −0.19 eV for Cs, Rb, and K-compounds, respectively, were applied to the subsequent optical property calculations.

The total and partial densities of states (DOS and PDOS) are shown in Figure 6. In $Ba_3CsGa_5Se_{10}Cl_2$, the HVB is derived mainly from Se 4p states, whereas the LCB is composed of Se 4p and Ga 4s states mixed with small amount of Se 4s and Ba 5d states. The valence bands (VB) spanning over −15.0 to −10.0 eV originate predominately from Se 4s, Ba 5p, and Ga 3d states, and a small portion of Cl 3s and Ga 4s states. The VBs ranging from −10.0 to −4.0 eV are mostly formed by Se 4p, Cs 5p, and Ga 4s states hybridized with small amounts of Se 4s and Cl 3p states. The VBs from −4.0 eV to the Fermi level (E_F) are

dx.doi.org/10.1021/ja209711x | J. Am. Chem.Soc. 2012, 134, 2227−2235

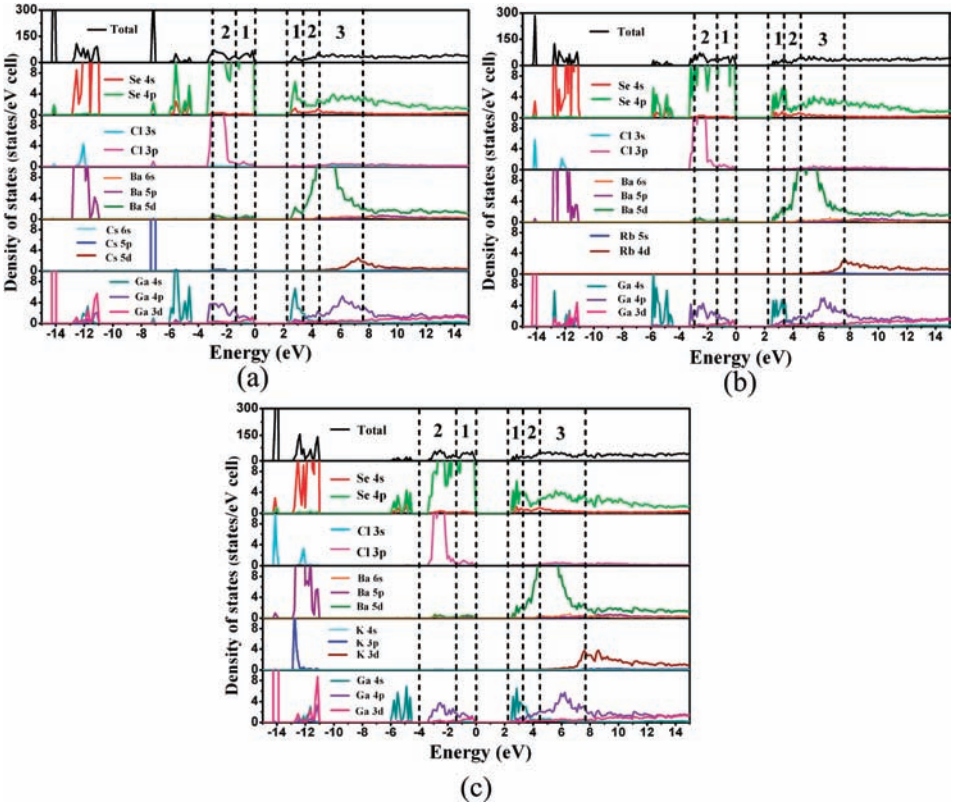

Figure 6. Total and partial densities of states of $Ba_3AGa_5Se_{10}Cl_2$ (A = Cs, Rb, and K). Dotted line and number mark the different regions in VB and CB.

mostly contributions of Se 4p, Cl 3p, and Ga 4p states with small amount of Ga 3d state. The Se 4p, Ba 5d, Ga 4s, and Ga 4p states mixing with a small amount of Se 4s state make up the conduction bands (CB) between E_F up to 6.0 eV. The CBs ranging from 6.0 to 15.0 eV mainly consist of Se 4p, Ba 5d, Cs 5d, and Ga 4p states with a small portion of Ga 3d. Similar DOS and PDOS are found for Rb and K-compounds. Briefly, the energy gaps are mainly determined by the skeleton Se and Ga atoms, i.e., the non-bonding state of Se 4p and the antibonding states of Ga 4s and Se 4p, therefore, the three title compounds have similar E_g, which agrees with the experimental results.

Optical Property Calculations. The linear optical properties were examined according to the complex dielectric function $\varepsilon(\omega) = \varepsilon_1(\omega) + i\varepsilon_2(\omega)$. The energy dependence of the real part ε_1 and imaginary part ε_2 are displayed in SI Figure S7–9. Because of the nonmetallic characteristics of the title compounds, the imaginary part $\varepsilon_2(\omega)$ is used to describe the interband electronic transitions between the occupied and unoccupied states. The average values of the polarized zero-frequency dielectric constants $\varepsilon_1^{ave}(0)$ are 6.74, 6.58, and 6.61 for Cs, Rb and K-compounds, respectively. The calculated basic absorption edges are 2.0, 2.1, and 2.1 eV, which are comparable with the experimental results. The dominating peaks of the imaginary part $\varepsilon_2(\omega)$ locating around 4.8, 4.9, and 4.9 eV can be mainly assigned to the interband electronic transitions from Se 4p states to Se 4p and Ga 4s states for Cs, Rb, and K-compounds, respectively. The refractive index $n(\omega)$, birefringence (Δn), absorption coefficient $I(\omega)$ and reflectivity $R(\omega)$ were also calculated according to the formulas (1–4):

$$n(\omega) = \sqrt{\frac{\sqrt{\varepsilon_1^2(\omega) + \varepsilon_2^2(\omega)} + \varepsilon_1}{2}} \quad (1)$$

$$\Delta n = |n_i - n_j|_{max} (i, j = 1, 2, 3; i \neq j) \quad (2)$$

$$I(\omega) = \frac{2\omega\kappa(\omega)}{c} (\kappa = \text{the extinction coefficient}) \quad (3)$$

$$R(\omega) = \frac{(n-1)^2 + \kappa^2}{(n+1)^2 + \kappa^2} (n\text{: refractive index}) \quad (4)$$

As shown in SI Figure S10, the static refractive indexes are 2.59, 2.56, and 2.57, for Cs, Rb, and K-compounds, respectively. The reflectivity $R(\omega)$ in the range of 0–14 eV, is less than 40% which suggests a good photopermeability. (SI Figure S11) The highest absorption peaks locate around 17.5 eV (i.e., 3.2×10^5 cm^{-1}, SI Figure S12). As plotted in SI Figure S13, the static birefringence (Δn) are found to be very small, 0.011, 0.006, and 0.007 for Cs, Rb and K-compounds, which are smaller than that of $AgGaS_2$ (0.048). The highest Δn values, 0.24, 0.32, and 0.36, are located around 2.52, 4.01, and 4.01 eV, respectively. The relatively small Δn values in the IR region (<2.0 eV) indicate non phase-matchable behaviors, which are consistent with the experimental observations. However, larger Δn values are suggested in other energy regions, which indicates that the title compounds may be phase matchable in higher energy regions.

The rank n second-order susceptibility tensor X^n in $\bar{4}$ symmetry has 4 nonvanishing elements: χ_{14}, χ_{15}, χ_{31} and χ_{36}, only two of which remain in the low-energy region and under the assumption of Kleinman symmetry ($\chi_{14} = \chi_{36}$, $\chi_{15} = \chi_{31}$). Because of the disorder of Ba and alkali metal atoms in the title

dx.doi.org/10.1021/ja209711x | J. Am. Chem.Soc. 2012, 134, 2227–2235

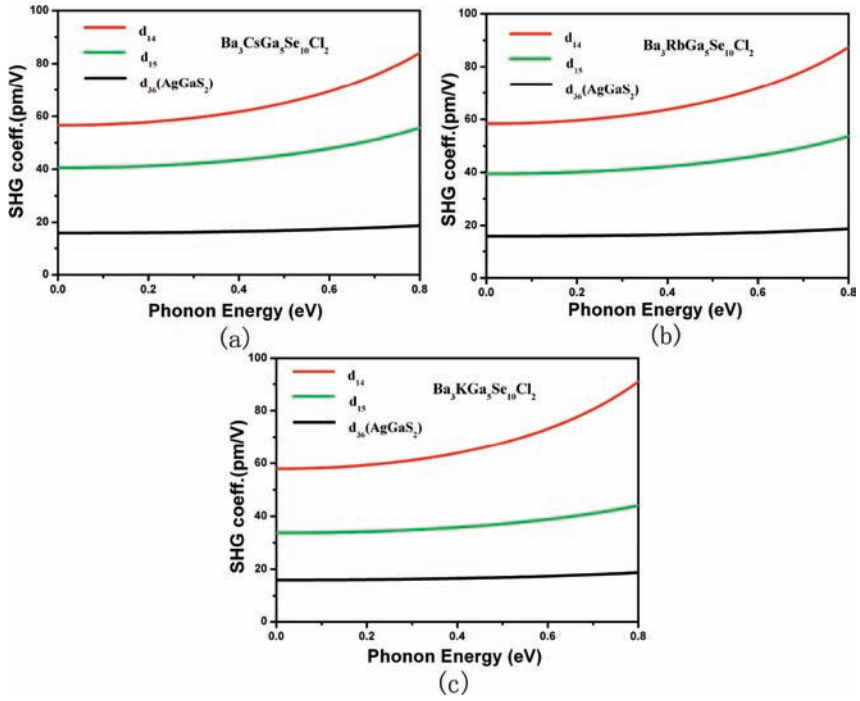

Figure 7. Calculated frequency-dependent second harmonic generation coefficients for $Ba_3AGa_5Se_{10}Cl_2$ (A = Cs, Rb and K).

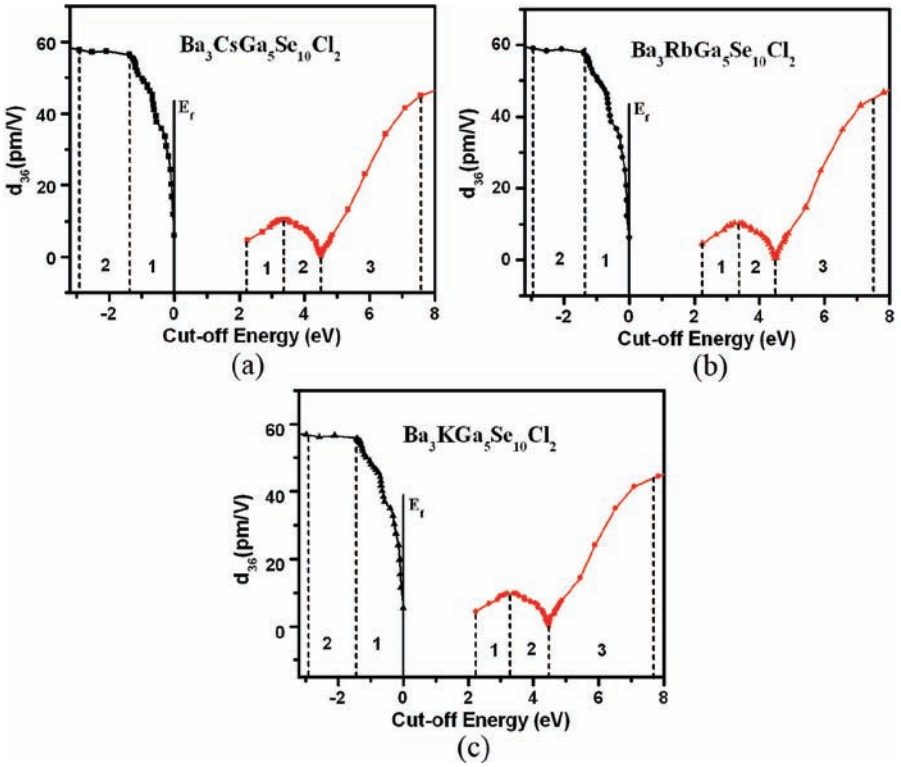

Figure 8. Cutoff-energy-depending static SHG coefficients for $Ba_3AGa_5Se_{10}Cl_2$ (A = Cs, Rb, and K). Dotted line and number mark the different regions in VB and CB.

compounds, a model with *P*1 symmetry was built as described above, in which ten independent second-order tensors exist under the restriction of Kleinman symmetry (χ_{11}, χ_{12}, χ_{13}, χ_{14}, χ_{15}, χ_{16}, χ_{22}, χ_{23}, χ_{24}, and χ_{33}), of which, χ_{14} and χ_{15} that are twice the SHG coefficient d_{14} or d_{15} are studied. As shown in Figure 7, the calculated d_{14} and d_{15} coefficients are 69.85, 72.54, 73.29 pm/V and 47.68, 46.52, 39.31 pm/V, for Cs, Rb, and K-compounds, respectively, at the wavelength of 2.05 μm (0.61 eV). In comparison, the d_{36} for $AgGaS_2$ (17.6 pm/V) is significantly small, which is in accordance with the experimental observations.

The cutoff-energy dependence of the static SHG coefficient (d_{14}) is studied to explore the source of the SHG response. As shown in Figures 8 and SI S14, the origin of the SHG response

dx.doi.org/10.1021/ja209711x | *J. Am. Chem.Soc.* 2012, 134, 2227−2235

is dominated by VB-1 and CB-3 region. The VB-1 is dominated by Se 4p states hybridized with a small amount of Cl 3p, Ga 4p, and Ga 3d, whereas the CB-3 is mainly contributed from the Ba 5d states mixing with small amounts of Se 4p, Cs 5d, and Ga 4p. Consequently, the SHG response may be ascribed to the electronic transitions from Se 4p, Cl 3p, Ga 4p, and Ga 3d to Ba 5d, Se 4p, Cs 5d/Rb 4d/K 3d, and Ga 4p.

CONCLUSIONS

Novel inorganic open-framework chalcohalides with strong SHG intensities, $Ba_3AGa_5Se_{10}Cl_2$ (A = Cs, Rb, and K), have been discovered via solid state reactions. The supertetrahedral framework features a zinc-blende topological structure in which Zn and S sites are alternately substituted by T2 supertetradedral $Ga_4Se_{10}^{8-}$ cluster and T1 GaS_4^{5-} tetrahedron, and Ba/A cations and Cl anions locate in the cavities. Remarkably, these represent the first supertetrahedral open-framework structure exhibiting strong SHG intensities about 100, 20, and 10 times that of commercial $AgGaS_2$ at 2.05 μm in the particle size of 30−46 μm for Cs, Rb, and K-compound, respectively. These compounds show wide MFIR optical transparency regions (0.89−25, 0.65−25, and 0.86−25 μm). In addition, the title compounds also represent the first open-framework compound with outstanding red emission photoluminescent properties. These polar open-framework chalcohalides provide a new opportunity to design multifunctional materials that simultaneously exhibit SHG and photoluminescence property. Extended works on other noncentrosymmetric chalcohalides are worth of trying.

ASSOCIATED CONTENT

Supporting Information

The additional crystallographic data, CIF files, XRD patterns, reflection and FT-IR spectra, UV diffuse reflectance spectra, the calculation results including dielectric functions, refractive index, reflectivity, absorption coefficient, and birefringence, together with a complete ref 14. This material is available free of charge via the Internet at http://pubs.acs.org.

AUTHOR INFORMATION

Corresponding Author

chenl@fjirsm.ac.cn.

ACKNOWLEDGMENTS

This research was supported by the National Natural Science Foundation of China under Projects (90922021, 21171168, 20973175), the "Knowledge Innovation Program of the Chinese Academy of Sciences" (KJCX2-YW-H20). We thank Prof. Ning Ye and Dr. Xin-Song Lin at FJIRSM for help with the SHG measurements, and Prof. Yong-Fan Zhang at Fuzhou University for help with SHG calculations.

REFERENCES

(1) Shunemann, C. P. *Proc. SPIE-Int. Soc. Opt. Eng.* **2007**, *6455*, 64550R−1.
(2) Bordui, P. F.; Fejer, M. M. *Annu. Rev. Mater. Sci.* **1993**, *23*, 321.
(3) Hazama, H.; Takatani, Y.; Awazu, K. *Proc. SPIE-Int. Soc. Opt. Eng.* **2007**, *6455*, 645507−1.
(4) Chen, C. T.; Wu, B. C.; Jiang, A. D.; You, G. M. *Sci. Sin. B.* **1985**, *28*, 235.
(5) Chen, C. T.; Wu, Y. C.; Jiang, A. D.; Wu, B. C.; You, G. M.; Li, R. K.; Lin, S. J. *J Opt. Soc. Am. B.* **1989**, *6*, 616.
(6) Wu, Y. C.; Sasaki, T.; Nakai, S.; Yokotani, A.; Tang, H. G.; Chen, C. T. *Appl. Phys. Lett.* **1993**, *62*, 2614.
(7) Mori, Y.; Kuroda, I.; Nakajima, S.; Sasaki, T.; Nakai, S. *Appl. Phys. Lett.* **1995**, *67*, 1818.
(8) Sasaki, T.; Mori, Y.; Kuroda, I.; Nakajima, S.; Yamaguchi, K.; Watanabe, S.; Nakai, S. *Acta. Crystallogr. C.* **1995**, *51*, 2222.
(9) Tu, J. M.; Keszler, D. A. *Mater. Res. Bull.* **1995**, *30*, 209.
(10) Eckardt, R. C.; Masuda, H.; Fan, Y. X.; Byer, R. L. *IEEE J. Quantum Electon.* **1990**, *26*, 922.
(11) Bergman, J. G.; Crane, G. R. *J. Solid. State. Chem.* **1975**, *12*, 172.
(12) Sun, C. F.; Hu, C. L.; Xu, X.; Ling, J. B.; Hu, T.; Kong, F.; Long, X. F.; Mao, J. G. *J. Am. Chem. Soc.* **2009**, *131*, 9486.
(13) Ra, H. S.; Ok, K. M.; Halasyamani, P. S. *J. Am. Chem. Soc.* **2003**, *125*, 7764.
(14) Fossier, S.; et al. *J. Opt. Soc. Am. B* **2004**, *21*, 1981.
(15) Panyutin, V.; Badikov, V.; Shevyrdyaeva, G.; Mitin, K.; Seryogin, A.; Petrov, V.; Noack, F. *Proc. SPIE-Int. Soc. Opt. Eng.* **2008**, *6875*, 68750A−1.
(16) Bhar, G. C. *Jpn. J. Appl. Phys.* **1993**, *32*, 653.
(17) Boyd, G. D.; Kasper, H. Mcfee, J. H. *IEEE J. Quantum Electron.* **1971**, QE 7, *12*, 563.
(18) Harasaki, A.; Kato, K. *Jpn. J. Appl. Phys.* **1997**, *36*, 700.
(19) Tell, B.; Kasper, H. M. *Phys. Rev. B.* **1971**, *4*, 4455.
(20) Kasper, H. M. *J. Electrochem. Soc.* **1972**, *119*, C96.
(21) Airoldi, G.; Beucherie, P.; Rinaldi, C. *J. Cryst. Growth.* **1977**, *38*, 239.
(22) Boyd, G. D.; Buehler, E.; Storz, F. G. *Appl. Phys. Lett.* **1971**, *18*, 301.
(23) Petrov, V.; Yelisseyev, A.; Isaenko, L.; Lobanov, S.; Titov, A.; Zondy, J. J. *Appl. Phys. B-Lasers. O* **2004**, *78*, 543.
(24) Kish, Z. Z.; Loshchak, V. V.; Peresh, E. Y.; Semrad, E. E. *Inorg. Mater.* **1989**, *25*, 1658.
(25) Atuchin, V. V.; Lin, Z.; Isaenko, L. I.; Kesler, V. G.; Kruchinin, V. N.; Lobanov, S. I. *J. Phys.: Condens. Matter.* **2009**, *21*, 455502.
(26) Lin, X. S.; Zhang, G.; Ye, N. *Cryst. Growth. Des.* **2009**, *9*, 1186.
(27) Yao, J. Y.; Mei, D. J.; Bai, L.; Lin, Z. S.; Yin, W. L.; Fu, P. Z.; Wu, Y. C. *Inorg. Chem.* **2010**, *49*, 9212.
(28) Kim, Y.; Seo, I. S.; Martin, S. W.; Baek, J.; Halasyamani, P. S.; Arumugam, N.; Steinfink, H. *Chem. Mater.* **2008**, *20*, 6048.
(29) Liao, J. H.; Marking, G. M.; Hsu, K. F.; Matsushita, Y.; Ewbank, M. D.; Borwick, R.; Cunningham, P.; Rosker, M. J.; Kanatzidis, M. G. *J. Am. Chem. Soc.* **2003**, *125*, 9484.
(30) Chung, I.; Malliakas, C. D.; Jang, J. I.; Canlas, C. G.; Weliky, D. P.; Kanatzidis, M. G. *J. Am. Chem. Soc.* **2007**, *129*, 14996.
(31) Bera, T. K.; Jang, J. I.; Ketterson, J. B.; Kanatzidis, M. G. *Abstracts of Papers of the American Chemical Society*; Springer: Washington, 2009.
(32) Bera, T. K.; Jang, J. I.; Ketterson, J. B.; Kanatzidis, M. G. *J. Am. Chem. Soc.* **2009**, *131*, 75.
(33) Das, S.; Chatterjee, U.; Ghosh, C.; Gangopadhyay, S.; Andreev, Y. M.; Lanskii, G.; Badikov, V. V. *Opt. Commun.* **2006**, *259*, 868.
(34) Zhang, J.; Seo, I. S.; Yang, C.; Qin, J. G.; Ye, N.; Wu, B. C.; Chen, C. T. *Proc. SPIE.* **1998**, 3556(1) Electro-Optic andSecond Harmonic GenerationMaterials, Devices, and Applications II, Beijing, P. R. China..
(35) Ren, P.; Qin, J. G.; Chen, C. T. *Inorg. Chem.* **2003**, *42*, 8.
(36) Zhang, G.; Qin, J. G.; Liu, T.; Zhu, T. X.; Fu, P. Z.; Wu, Y. C.; Chen, C. T. *Cryst. Growth. Des.* **2008**, *8*, 2946.
(37) Jiang, X. M.; Zhang, M. J.; Zeng, H. Y.; Guo, G. C.; Huang, J. S. *J. Am. Chem. Soc.* **2011**, *133*, 3410.
(38) Phanon, D.; Gautier-Luneau, I. *Angew. Chem., Int. Ed.* **2007**, *46*, 8488.
(39) Phanon, D.; Bentria, B.; Benbertal, D.; Mosset, A.; Gautier-Luneau, I. *Solid. State. Sci.* **2006**, *8*, 1466.
(40) Gitzendanner, R. L.; DiSalvo, F. J. *Inorg. Chem.* **1996**, *35*, 2623.
(41) Kanatzidis, M. G.; Zhang, Q.; Chung, I.; Jang, J. I.; Ketterson, J. B. *J. Am. Chem. Soc.* **2009**, *131*, 9896.
(42) Guo, S. P.; Guo, G. C.; Wang, M. S.; Zou, J. P.; Zeng, H. Y.; Cai, L. Z.; Huang, J. S. *Chem. Commun.* **2009**, 4366.

(43) Kim, M. K.; Kim, S. H.; Chang, H. Y.; Halasyamani, P. S.; Ok, K. M. *Inorg. Chem.* **2010**, *49*, 7028.
(44) Chen, M. C.; Li, L. H.; Chen, Y. B.; Chen, L. *J. Am. Chem. Soc.* **2011**, *133*, 4617.
(45) Kong, F.; Huang, S. P.; Sun, Z. M.; Mao, J. G.; Cheng, W. D. *J. Am. Chem. Soc.* **2006**, *128*, 7750.
(46) Becker, P. *Adv. Mater.* **1998**, *10*, 979.
(47) Do, J. H.; Kanatzidis, M. G. *J. Alloy. Compd.* **2004**, *381*, 41.
(48) Huang, Y. Z.; Wu, L. M.; Wu, X. T.; Li, L. H.; Chen, L.; Zhang, Y. F. *J. Am. Chem. Soc.* **2010**, *132*, 12788.
(49) Feng, P. Y. *Chem. Commun.* **2001**, 1668.
(50) Zheng, N. F.; Bu, X. H.; Feng, P. Y. *J. Am. Chem. Soc.* **2003**, *125*, 1138.
(51) Wang, C.; Bu, C.; Zheng, N. F; Feng, P. Y. *Angew. Chem., Int. Ed.* **2002**, *11*, 1959.
(52) Wang, C.; Li, Y. Q.; Bu, X. H.; Zheng, N. F.; Zivkovic, O.; Yang, C. S.; Feng, P. Y. *J. Am. Chem. Soc.* **2001**, *123*, 11506.
(53) Zheng, N. F.; Bu, X. G.; Wang, B.; Feng, P. Y. *Science.* **2002**, *298*, 2366.
(54) Zheng, N. F. *Science* **2003**, *299*, 1015.
(55) *CrystalClear*,v. 1.3.5; Rigaku Corp.: The Woodlands: TX, 1999.
(56) Sheldrick, G. M. *SHELXTL*,v. 5.1; Bruker-AXS: Madison, WI, 1998.
(57) Kortüm, G. *Reflectance Spectroscopy*; Springer-Verlag: New York, 1969.
(58) Kurtz, S. K.; Perry, T. T. *J. Appl. Phys.* **1968**, *39*, 3798.
(59) Kresse, G. *J. Non-Cryst. Solids.* **1995**, *193*, 222.
(60) Takeuchi, N.; Garzon, I. L. *Phys. Rev. B.* **1994**, *50*, 8342.
(61) Kresse, G.; Furthmuller, J. *Phys. Rev. B* **1996**, *54*, 11169.
(62) Perdew, J. P.; Burke, K.; Ernzerhof, M. *Phys. Rev. Lett.* **1996**, *77*, 3865.
(63) Perdew, J. P.; Wang, Y. *Phys. Rev. B.* **1992**, *45*, 13244.
(64) Lin, J. S.; Qteish, A.; Payne, M. C.; V, H. *Phys. Rev. B.* **1993**, *47*, 4174.
(65) Laksari, S.; Chahed, A.; Abbouni, N.; Benhelal, O.; Abbar, B. *Comput. Mater. Sci.* **2006**, *38*, 223.
(66) Mo, S. D.; Ching, W. *Phys. Rev. B.* **1995**, *51*, 13023.
(67) Aversa, C.; Sipe, J. E. *Phys. Rev. B.* **1995**, *52*, 14636.
(68) Rashkeev, S. N.; Lambrecht, W. R. L.; Segall, B. *Phys. Rev. B* **1998**, *57*, 3905.
(69) Lubbers, D.; Leute, V. *J. Solid. State. Chem.* **1982**, *43*, 339.
(70) Isaenko, L.; Yelisseyev, A.; Lobanov, S.; Titov, A.; Petrov, V.; Zondy, J. J.; Krinitsin, P.; Merkulov, A.; Vedenyapin, V.; Smirnova, J. *Cryst. Res. Technol.* **2003**, *38*, 379.
(71) Wang, C.; Bu, X. H.; Zheng, N. F.; Feng, P. Y. *J. Am. Chem. Soc.* **2002**, *124*, 10268.
(72) Trikalitis, P. N.; Tsamourtzi, K.; Song, J. H.; Bakas, T.; Freeman, A. J.; Kanatzidis, M. G. *Inorg. Chem.* **2008**, *47*, 11920.
(73) Poulsen, N. J. *Mater. Res. Bull.* **1998**, *33*, 313.
(74) Kleinke, H.; Assoud, A. *Solid. State. Sci.* **2010**, *12*, 919.
(75) Bhar, G. C.; Smith, R. C. *Phys. Status. Solidi. A* **1972**, *13*, 157.
(76) Li, P.; Li, L. H.; Chen, L.; Wu, L. M. *J. Solid. State. Chem.* **2010**, *183*, 444.
(77) Ok, K. M.; Chi, E. O.; Halasyamani, P. S. *Chem. Soc. Rev.* **2006**, *35*, 710.
(78) Kurtz, S. K.; Perry, T. T. *J. Appl. Phys.* **1968**, *39*, 3798.
(79) Muller, E. A.; Cannon, R. J.; Sarjeant, A. N.; Ok, K. M.; Halasyamani, P. S.; Norquist, A. J. *Cryst. Growth. Des.* **2005**, *5*, 1913.
(80) Nikogosyan, D. N. *Nonlinear Optical Crystals: A Complete Survey*; Springer: New York, 2005.
(81) You, S. H.; Hong, K. J.; Jeong, T. S.; Youn, C. J. *J. Appl. Phys.* **2010**, *108*, 053520.